IEEE Access
Multidisciplinary | Rapid Review | Open Access Journal

Received 19 April 2023, accepted 12 May 2023, date of publication 17 May 2023, date of current version 25 May 2023.

Digital Object Identifier 10.1109/ACCESS.2023.3277252

RESEARCH ARTICLE

0.5-V Nano-Power Voltage-Mode First-Order Universal Filter Based on Multiple-Input OTA

FABIAN KHATEB[1,2,3], MONTREE KUMNGERN[4], AND TOMASZ KULEJ[5]

[1]Department of Microelectronics, Brno University of Technology, 601 90 Brno, Czech Republic
[2]Faculty of Biomedical Engineering, Czech Technical University in Prague, 272 01 Kladno, Czech Republic
[3]Department of Electrical Engineering, Brno University of Defence, 662 10 Brno, Czech Republic
[4]Department of Telecommunications Engineering, School of Engineering, King Mongkut's Institute of Technology Ladkrabang, Bangkok 10520, Thailand
[5]Department of Electrical Engineering, Częstochowa University of Technology, 42-201 Czestochowa, Poland

Corresponding author: Montree Kumngern (montree.ku@kmitl.ac.th)

This work was supported by the University of Defence Brno within the Organization Development Project Varops.

ABSTRACT This paper presents a new application of the multiple-input operational transconductance amplifier (MI-OTA). The MI-OTA has been used to realize a first-order universal filter which shows that the first-order transfer functions such as low-pass, high-pass, and all-pass filters can be obtained easily from a single topology by applying the input signal to the appropriate terminals. Moreover, both non-inverting and inverting transfer functions of all filtering functions can be obtained. The pole frequency of all filters can also be controlled electronically. The first-order all-pass filters have been selected to realize high-quality band-pass filter. For low-voltage supply operation and extremely low power consumption, the proposed MI-OTA is realized by the multiple-input bulk-driven MOS transistor technique with transistors operating in subthreshold voltage region. The circuit has been simulated using the 0.18 μm TSMC CMOS technology with 0.5 V of supply voltage and it consumes 29.77 nW of power for 10 nA nominal setting current. The post-layout simulation results show that the applications of MI-OTA agree well with theory.

INDEX TERMS Analog filter, operational transconductance amplifier, analog circuit, low-voltage, low-power CMOS.

I. INTRODUCTION

For first-order filters, there are three filtering functions that are possible for realization, namely low-pass filter (LPF), high-pass filter (HPF), and all-pass filter (APF). The LPF and HPF are the well-known networks that can be applied to electronic, communication and control systems. The first-order LPF and first-order HPF, the so-called lossy integrator and lossy differentiator, can be used to realize high-order filters such odd-order filters that cascaded using biquads [1], and proportional-integral-derivative (PID) controller [2]. The APFs, the so-called phase shifter circuits, are the network that passes all frequencies equally in magnitude, but its phase relationship is changed along with variation of the frequencies. The first-order APF can be applied to realize high-quality (Q) factor band-pass filter (BPF) [3], quadrature oscillator, and multiphase oscillator [4]. There are many universal filters that can realize first-order APF, LPF, and HPF into a single topology available in open literature [5], [6], [7], [8], [9], [10], [11], [12], [13], [14], [15], [16], [17], [18], [19], [20], [21], [22], [23], [24], [25], [26], [27], [28], [29], [30], [31], [32], [33], [34], [35], [36], [37], [38], [39]. These first-order universal filters can be classified into three mode-operations, namely current-mode (CM) circuits [5], [6], [7], [8], [9], [10], [11], [12], [13], [14], [15], [16], [17], [18], [19], [20], voltage-mode (VM) circuits [21], [22], [23], [24], [25], [26], [27], [28], [29], [30], [31], [32], [33], [34], and mixed-mode (MM) circuits [35], [36], [37], [38], [39].

This work is focused on VM filter that should offer high-input and low-output impedance. Considering first-order universal filters in [5], [6], [7], [8], [9], [10], [11], [12], [13], [14], [15], [16], [17], [18], [19], [20], [21], [22], [23], [24], [25], [26], [27], [28], [29], [30], [31], [32], [33], [34], [35], [36], [37], [38], and [39], only CM universal filters in [5] and [14] can realize six first-order transfer functions into single topology, namely non-inverting of LPF, HPF, APF,

The associate editor coordinating the review of this manuscript and approving it for publication was Dušan Grujić.

This work is licensed under a Creative Commons Attribution-NonCommercial-NoDerivatives 4.0 License.
For more information, see https://creativecommons.org/licenses/by-nc-nd/4.0/

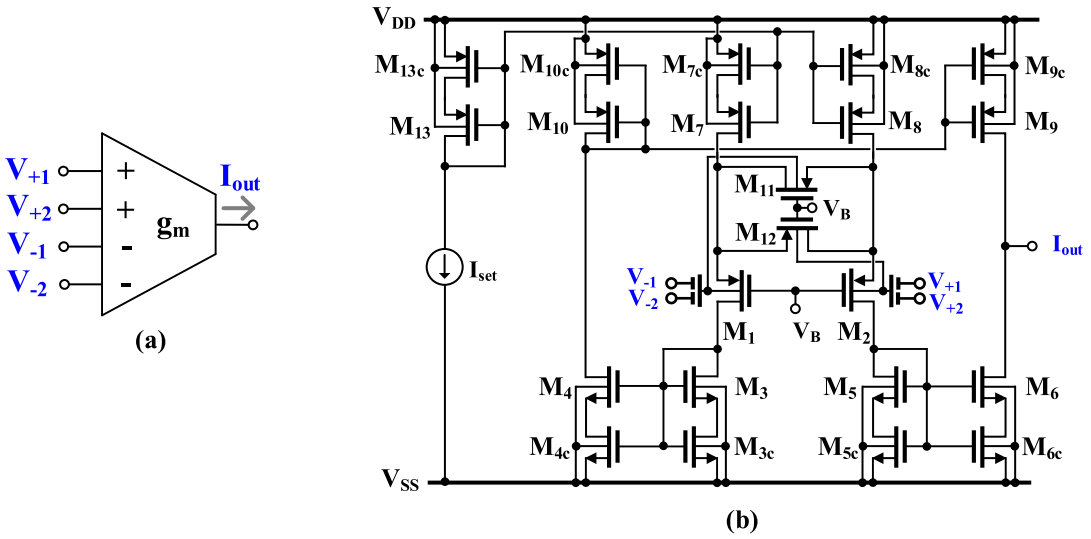

FIGURE 1. Electrical symbol of MI-OTA (a) and its schematic based on multiple-input bulk-driven differential pair with source degeneration transistors (b).

and inverting of LPF, HPF, APF. These CM filters are realized based on multiple-output active devices such as current follower transconductance amplifier (CFTA) [5] and inverting second-generation current conveyors (ICCIIs) [14]. However, the use of multiple-output current of active device-based circuits results in high power consumptions. The MM filters in [35], [36], [37], [38], and [39] can provide several first-order transfer functions but the transfer functions of CM, VM, trans-admittance (TAM), trans-impedance (TIM) of MM filters in [35], [36], [37], [38], and [39] do not provide both non-inverting and inverting output signals. Some filters such as [39] the input signal is applied via capacitor which is not ideal for VM circuits. Considering VM filters in [21], [22], [23], [24], [25], [26], [27], [28], [29], [30], [31], [32], [33], and [34], there is no first-order filters that can realize both non-inverting and inverting transfer functions of LPF, HPF and APF into a single circuit. The filters with available non-inverting and inverting transfer functions may be offered easily for applications such as cascaded of non-inverting and inverting APFs for realizing high-Q band-pass filters [40], for multiphase sinusoidal oscillator [41], [42], without additional circuits. The multiple-input voltages of devices can provide the advantages such as reduced number of active blocks for applications [43], [44], that result to minimum power consumption.

This work a new application of 0.5 V multiple-input OTA to first-order universal filter has been proposed. The multiple-input OTA can be easily obtained using multiple-input bulk-driven MOS transistor (MI-BD MOST) technique that increase the number of input terminals without increasement of the power consumption of OTA. To show the advantages of multiple-input OTA, it has been used to realize first-order VM universal filter. Unlike previous VM universal filters, the proposed universal filter provides six first-order transfer functions into single topology, namely non-inverting of LPF, HPF, APF and inverting of LPF, HPF, APF. The pole frequency of all filters can be controlled electronically. The proposed filters have been used to realized high-Q band-pass filter to confirm the new circuit.

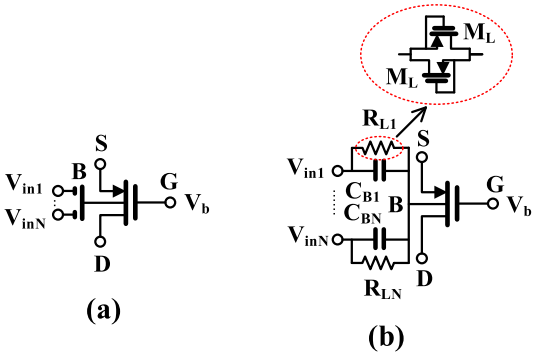

FIGURE 2. Symbol of MI-BD MOS transistor (a) and its realization (b).

II. PROPOSED CIRCUIT

A. MULTIPLE-INPUT OTA

The symbol of the multiple-input OTA (MI-OTA) is shown in Fig. 1 (a) and its transfer characteristic in ideal case can be expressed by:

$$I_{out} = g_m (V_{+1} + V_{+2} - V_{-1} - V_{-2}) \quad (1)$$

where g_m is the transconductance gain, V_{+1} and V_{+2} are the non-inverting input voltages, V_{-1} and V_{-2} are the inverting input voltages, and I_{out} is the output current.

Fig. 1 (b) shows the CMOS implementation of the MI-OTA based on multiple-input bulk-driven differential pair with source degeneration transistors, which was experimentally verified and first presented in [45]. The differential pair is based on multiple-input bulk-driven technique (MI-BD).

The electrical symbol of the MI-BD MOS transistor and its realization are shown in Fig. 2 (a) and (b), respectively. The device consists of a BD MOS transistor and a capacitive voltage divider/analog summing circuit, composed of capacitors C_{Bi}. In general case i = 1... N, but for the particular realization applied in this work N = 2. The capacitors are shunted with large resistances R_{Li}, that provides proper biasing of the bulk terminal of the MI-BD MOS for DC. The resistances are realized as anti-parallel connection of two minimum-size MOS transistors M_L operating in cutoff region, that provides sufficiently high resistance with minimum silicon area. For frequencies larger than $1/2\pi R_{Li}C_{Bi}$, the capacitors dominate over the resistances, and assuming the input capacitance of the MOS transistor seen from the bulk terminal is much less than C_{Bi}, the voltage V_b at the bulk terminal of MI-BD MOS can be expressed as:

$$V_b = \sum_{i=1}^{N} \frac{C_{Bi}}{C_{\sum}} V_i \tag{2}$$

where $C_{\sum}$ is the sum of all capacitances C_B.

Overall, the OTA in Fig.1(b) use a typical current mirror topology. Its input differential pair is composed of MI-BD MOS transistors M_1 and M_2. Note, that except increasing the number of inputs, the capacitive voltage divider discussed above increases the input linear range of the OTA. The input linear range is further increased using the BD transistors M_{11}, M_{12}, which operate in triode region, and act as source degenerative resistors. Note, that the bulk terminals of M_1 and M_{11} (M_2 and M_{12}) are tied together, which allows maintaining the same V_{BS} voltages for M_1-M_2 and M_{11}-M_{12} with common-mode variations, while the same V_{GS} voltages are provided by connecting all gates of the above transistors to the auxiliary biasing voltage V_B. This allows maintaining constant relationship of transconductances of the above transistors, even for variations of the common-mode voltage. Similar solution is known for conventional gate-driven (GD) transistors [46], [47], however, here, the BD devices are used. It can be shown that optimum linearity of the circuit is achieved when the following condition is met:

$$k = \frac{(W/L)_{11,12}}{(W/L)_{1,2}} = 0.5 \tag{3}$$

where W and L are the channel width and length respectively: This condition is the same as for the gate driven counterpart of the input pair, operating in a weak inversion region [47].

Assuming that current gain of all current mirrors in the OTA structure is equal to unity, all capacitors C_B are equal to each other, and neglecting other second order effects, the OTA transconductance can be expressed as:

$$g_m \cong \frac{1}{2}\eta \cdot \frac{4k}{4k+1} \cdot \frac{I_{set}}{n_p U_T} \tag{4}$$

where $\eta = g_{mb1,2}/g_{m1,2}$is the bulk to gate transconductance ratio for the input transistors M_1 and M_2, n_p is the subthreshold slope factor for p-channel MOS transistors, U_T is the thermal potential and I_{set} is the biasing current, which can be used to tune the value of g_m.

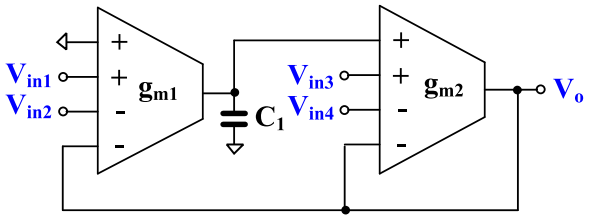

FIGURE 3. Proposed voltage-mode first-order universal filter.

The input capacitive divider, the bulk-driven technique, and the source-degenerative technique improve the circuit linearity and increase its linear range but lead to decreasing the voltage gain of the OTA. In order to increase this, gain the MOS transistors M_3-M_{13} were replaced by MOS composite self-cascode transistors, that allows increasing their output conductances, and consequently the voltage gain of the OTA, while not limiting the output swing of the circuit.

The output resistance of the OTA can be approximated as:

$$r_o \cong (g_{m6}r_{ds6}r_{ds6c}) \,||\, (g_{m9}r_{ds9}r_{ds9c}) \tag{5}$$

and its DC voltage gain for optimum case (k = 0.5), and with other assumptions made previously, is consequently given by:

$$A_v = g_m r_o = \frac{1}{3}\eta \cdot \frac{I_{set}}{n_p U_T} \left[(g_{m6}r_{ds6}r_{ds6c}) \,||\, (g_{m9}r_{ds9}r_{ds9c})\right] \tag{6}$$

thus, as mentioned earlier, the voltage gain is improved thanks to the self-cascode connections.

The input-referred noise of the MI-OTA, referred to one of the differential inputs, can be expressed as:

$$\begin{aligned} \bar{v_n^2} = \frac{1}{g_m^2}\Bigg[& 2\bar{I_{n1,2}^2}\left(\frac{2g_{m11,12}}{g_{m1,2}+2g_{m11,12}}\right)^2 \\ & + 2\bar{I_{n7,8}^2}\left(\frac{g_{m1,2}}{g_{m1,2}+2g_{m11,12}}\right)^2 \\ & + \bar{I_{n11,12}^2}\left(2\frac{g_{m1,2}}{g_{m1,2}+2g_{m11,12}}\right)^2 + 4\bar{I_{n3-6}^2} + 2\bar{I_{n9,10}^2}\Bigg] \end{aligned} \tag{7}$$

where the noise currents $\bar{I_n^2}$ are:

$$\bar{I_{ni}^2} = 2qI_{Di} + \frac{1}{fC_{OX}}\left(\frac{Kg_{mi}^2}{W_i L_i}\right) \tag{8}$$

where I_{Di} is the drain current (in this design equal to I_{set}), C_{OX} is the oxide capacitance per unit area and K is the flicker noise constant (different for n- and p-channel transistors).

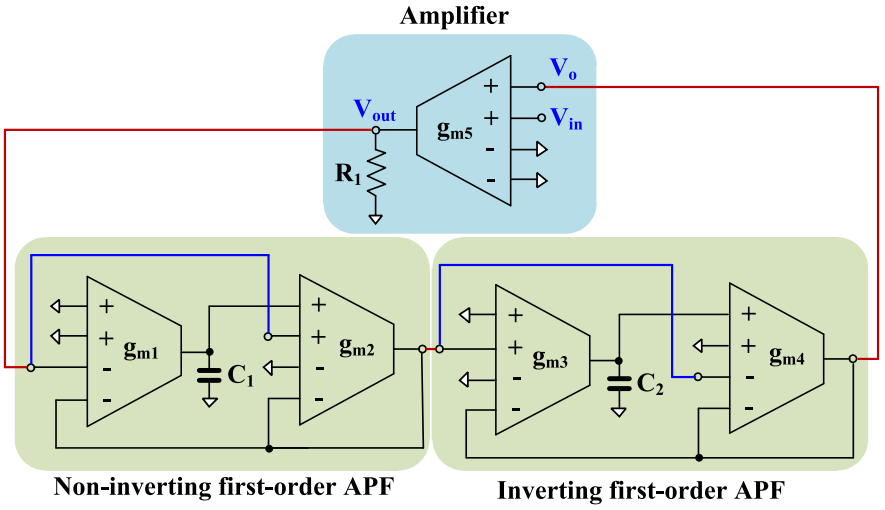

FIGURE 4. Proposed high-Q bandpass filter.

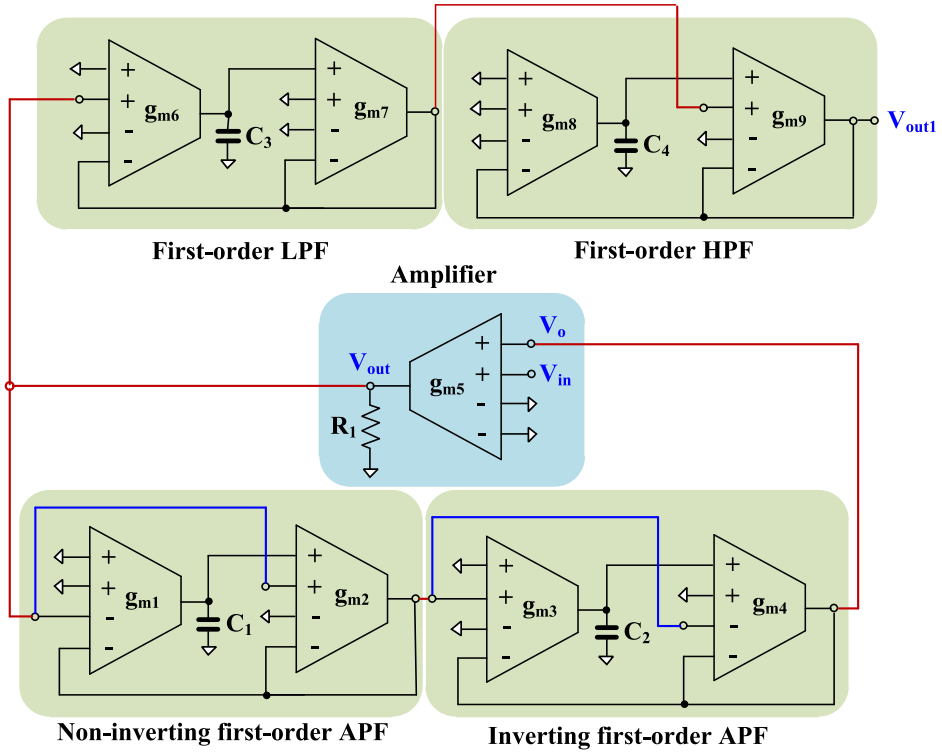

FIGURE 5. Improved high-Q bandpass filter.

As it can be concluded from (7), the input referred noise is increased due to the MI-BD technique, however, the input linear range is increased in the same proportion, thus, the resulting dynamic range remains the same, as for conventional OTA, based on a GD differential pair with source degeneration.

B. PROPOSED VOLTAGE-MODE FIRST-ORDER UNIVERSAL FILTER

Fig. 3 shows the proposed voltage-mode first-order universal filter. The circuit consists of two MI-OTAs and one grounded capacitor. It should be noted that the input voltages V_{in1}, V_{in2}, V_{in3}, and V_{in4} are supplied through the high-impedance

terminals of MI-OTAs, thus it requires no additional buffer circuits while the output impedance can be given by $1/g_{m2}$. Using (1) and nodal analysis, the output voltage of Fig. 3 can be expressed by:

$$V_o = \frac{sC_1\,(V_{in3} - V_{in4}) + g_{m1}\,(V_{in1} - V_{in2})}{sC_1 + g_{m1}} \tag{9}$$

The filtering functions of LPF, HPF, and APF can be obtained by appropriately applying the input signals with the condition expressed in Table 1.

It is evident that the proposed universal filter provides first-order transfer functions of non-inverting LPF, HPF, APF and inverting LPF, HPF, APF. Hence six transfer functions can be obtained into single topology which can be easily possible using MI-OTA that offers multiple-input non-inverting and inverting terminals.

The pole frequency of all filters can be given by:

$$\omega_o = \frac{g_{m1}}{C_1} \tag{10}$$

It is clear that the pole frequency can be controlled electronically by g_{m1} through the bias current I_{set1}.

TABLE 1. Obtaining Variant Filtering Functions Of The First-Order Universal Filter.

Filtering Function		Input	Transfer Function
LPF	Non-inverting	$V_{in1} = V_{in}$	$H(s) = \frac{g_{m1}}{sC_1 + g_{m1}}$
	Inverting	$V_{in2} = V_{in}$	$H(s) = -\frac{g_{m1}}{sC_1 + g_{m1}}$
HPF	Non-inverting	$V_{in3} = V_{in}$	$H(s) = \frac{sC_1}{sC_1 + g_{m1}}$
	Inverting	$V_{in4} = V_{in}$	$H(s) = -\frac{sC_1}{sC_1 + g_{m1}}$
APF	Non-inverting (Phase lag)	$V_{in4} = V_{in1} = V_{in}$	$H(s) = \frac{-sC_1 + g_{m1}}{sC_1 + g_{m1}}$
	Inverting (Phase lead)	$V_{in2} = V_{in3} = V_{in}$	$H(s) = \frac{sC_1 - g_{m1}}{sC_1 + g_{m1}}$

C. NON-IDEALITY ANALYSIS

Using non-idealities of OTA in [48], transconductance gain in the frequency range near its cut-off frequency can be expressed by

$$g_{mn} = g_m\,(1 - \mu s) \tag{11}$$

where $\mu = 1/\omega_g$ and ω_g is the first pole of the OTA. Using (11), (1) can be rewritten as

$$I_{out} = g_{mn}\,(V_{+1} + V_{+2} - V_{-1} - V_{-2}) \tag{12}$$

Using (12), the output voltage of Fig. 3 become

$$V_o = \frac{sC_1\,(V_{in3} - V_{in4}) + sC_1\left(1 - \frac{g_{m1}\mu_1}{C_1}\right) + g_{m1}\,(V_{in1} - V_{in2})}{sC_1\left(1 - \frac{g_{m1}\mu_1}{C_1}\right) + g_{m1}} \tag{13}$$

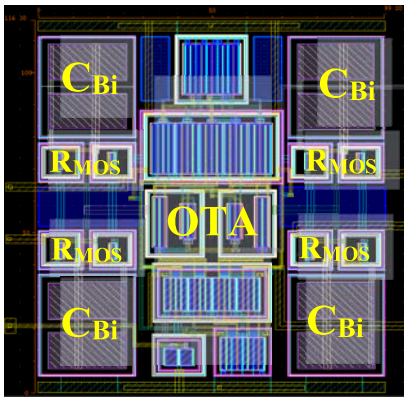

FIGURE 6. The layout of the MI-OTA.

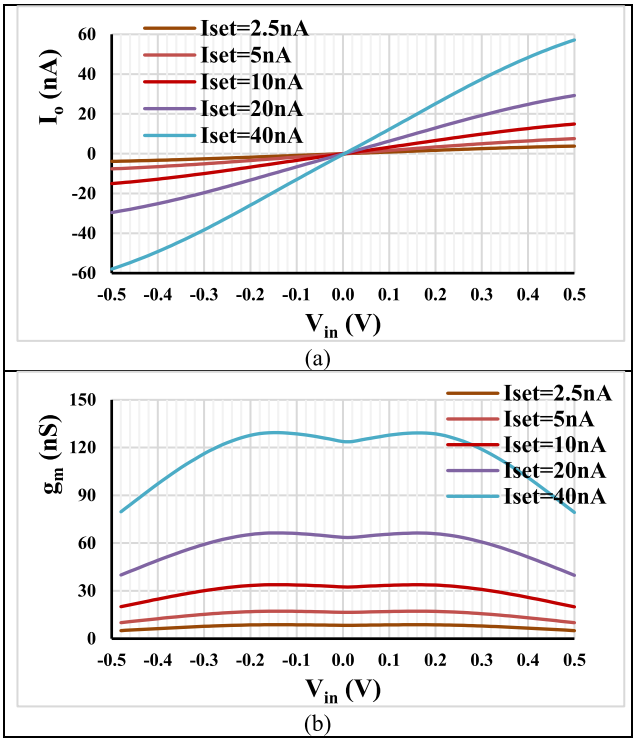

FIGURE 7. MI-OTA output current I_o (a) and transconductance g_m (b) versus V_{in} for different I_{set}.

It can be made negligible by satisfying the condition:

$$\frac{g_{m1}\mu_1}{C_1} \ll 1 \tag{14}$$

Considering the parasitic parameters using the modeling the non-idealities in the OTA in [48], the output resistance R_o and output resistance C_o are considered

$$V_o = \frac{sC_1' + G_{o1}\,(V_{in3} - V_{in4}) + g_{m1}\,(V_{in1} - V_{in2})}{sC_1' + G_{o1} + g_{m1}} \tag{15}$$

where $C_1' = C_1 + C_{o1}$, $G_{o1} = 1/R_{o1}$, C_{o1} and R_{o1} are respectively the parasitic capacitance and parasitic resistance of OTA_1.

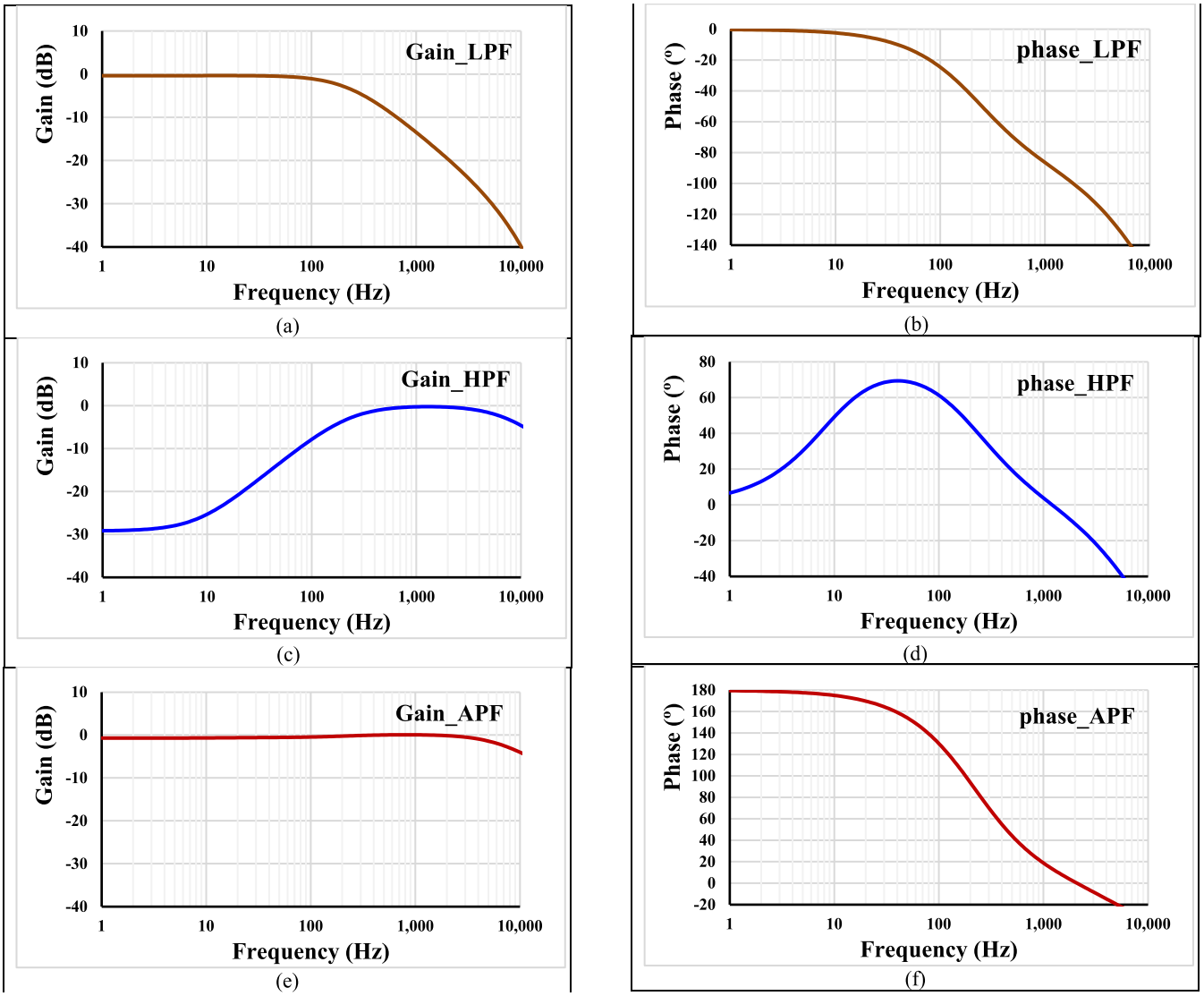

FIGURE 8. Frequency responses of gain and phase: (a,b) LPF; (c,d) HPF; (e,f) APF.

It should be noted that the parasitic capacitance effect of C_{o1} can be reduced by using the value of C_1 larger that the value of parasitic capacitance C_{o1} and the parasitic resistance effect of R_{o1} ($R_{o1} = 1/G_{o1}$) can be eliminated by using the value of g_{m1} greater that the value of parasitic resistance R_{o1}.

III. APPLICATION EXAMPLES

The proposed first-order universal filter has been used to realize a high-quality factor (high-Q) bandpass filter. To show the advantages of the proposed first-order universal filter, non-inverting and inverting first-order APFs that can realize into a single topology have been used. The transconductances g_{m1}, g_{m2} and C_1 realize the first APF, transconductances g_{m3}, g_{m4} and C_2 realize the second APF, and the transconductance g_{m5} and R_1 realize the amplifier. Considering amplifier section, the output voltage of amplifier can be given by

$$V_{out} = g_{m5}R_1 (V_{in} + V_o) \tag{16}$$

The output voltage V_{out} is applied to the input of the cascaded APF. Using the condition in Table 1, the output voltage V_o can be given by

$$V_o = -\left(\frac{sC_1 - g_{m1}}{sC_1 + g_{m1}}\right)\left(\frac{sC_2 - g_{m3}}{sC_2 + g_{m3}}\right) V_{out} \tag{17}$$

Letting $C_1 = C_2 = C$ and $g_{m1} = g_{m3} = g_m$, and substituting (17) to (16), we have

$$V_{out} = g_{m5}R_1 \left(V_{in} - \left(\frac{s^2C^2 - 2sCg_m + g_m^2}{s^2C^2 + 2sCg_m + g_m^2}\right) V_{out}\right) \tag{18}$$

The transfer function can be expressed by

$$\frac{V_{out}}{V_{in}} = \left(\frac{g_{m5}R_1}{1 + g_{m5}R_1}\right) \frac{(sC + g_m)^2}{s^2C^2 + 2sCg_m\left(\frac{1-g_{m5}R_1}{1+g_{m5}R_1}\right) + g_m^2} \tag{19}$$

This transfer function can be approximated as a bandpass transfer function near the center frequency [49].

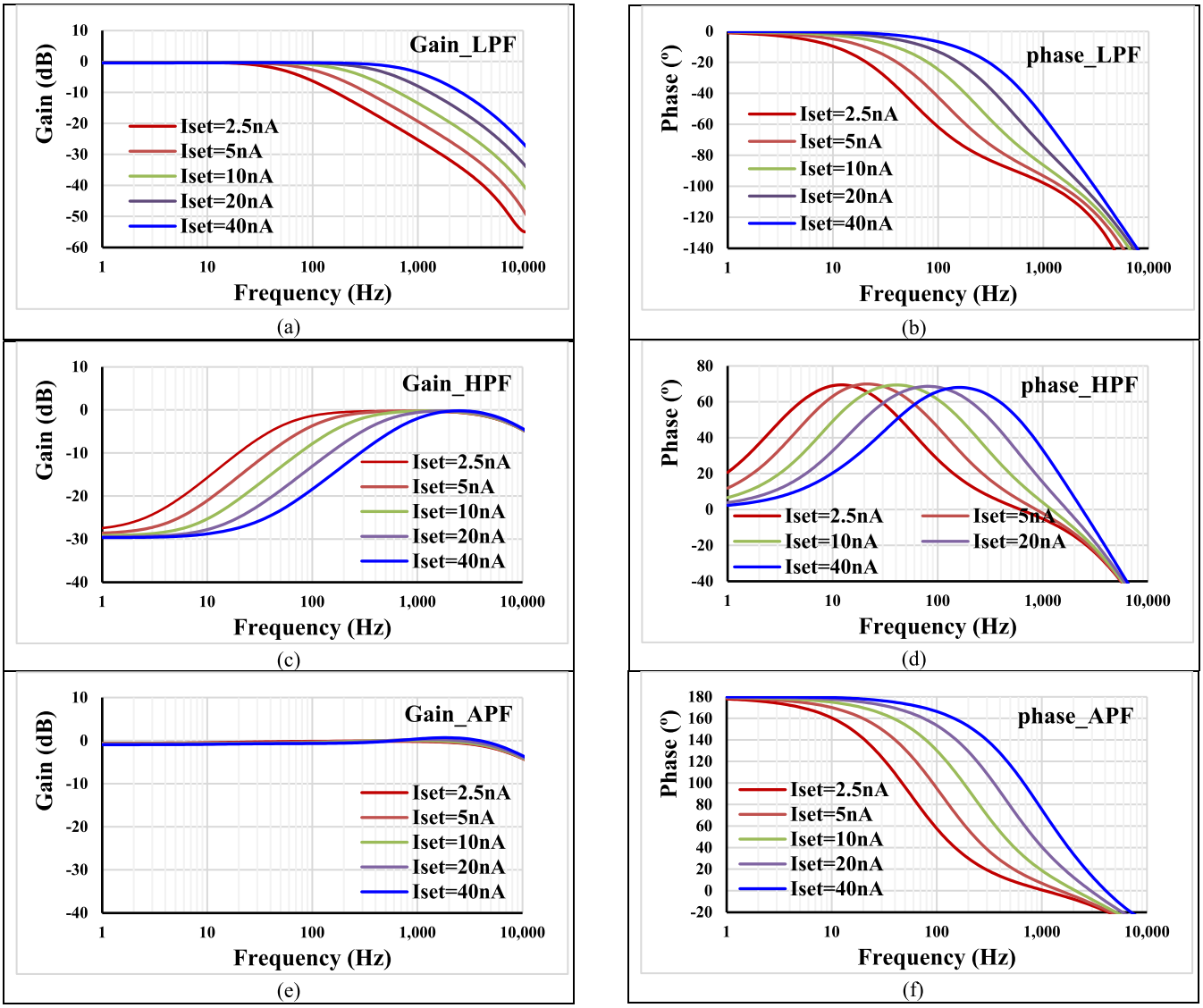

FIGURE 9. Frequency responses of gain and phase: (a,b) LPF; (c,d) HPF; (e,f) APF with different I_{set}.

The quality factor (Q) of bandpass filter can be given by

$$Q = \frac{1}{2}\left(\frac{1 + g_{m5}R_1}{1 - g_{m5}R_1}\right) \tag{20}$$

It is evident that the Q of filter can be adjusted be amplifier $g_{m5}R_1$ with the condition of $g_{m5}R_1 \ll 1$, which can be adjusted by g_{m5}.

Letting $g_m/C = \omega_o$ and using (20), (19) can be rewritten as

$$\frac{V_{out}}{V_{in}} = \frac{1}{4}(2Q - 1)\frac{\frac{(s+\omega_o)^2}{Q}}{s^2 + s\left(\frac{\omega_o}{Q}\right) + \omega_o^2} \tag{21}$$

Thus, approximated bandpass transfer function can be obtained.

It should be noted from (19) and (21) that the numerator of transfer function has double zero at a frequency ω_o which departs from an ideal bandpass filter that the zero is located at origin. If an ideal bandpass filter function is required, the output of Fig. 4 can be connected by cascaded first-order LPF and first-order HPF as shown in Fig. 5. From Fig. 5, using Table 1 and letting $g_{m6} = g_{m8} = g_m$, $C_3 = C_4 = C$, the output voltage V_{out1} can be given by

$$V_{out1} = \frac{sCg_m}{(sC + g_m)^2}V_{out} \tag{22}$$

Using (19), (22) become

$$\frac{V_{out1}}{V_{in}} = \left(\frac{g_{m5}R_1}{1 + g_{m5}R_1}\right)\frac{sCg_m}{s^2C^2 + 2sCg_m\left(\frac{1-g_{m5}R_1}{1+g_{m5}R_1}\right) + g_m^2} \tag{23}$$

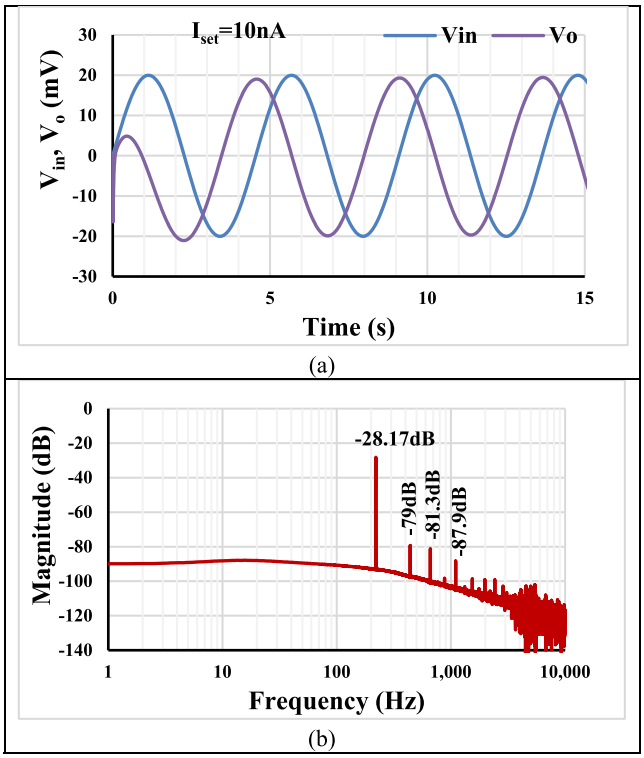

FIGURE 10. The transient response of the APF (a) and the spectrum of the Vo using FFT (b).

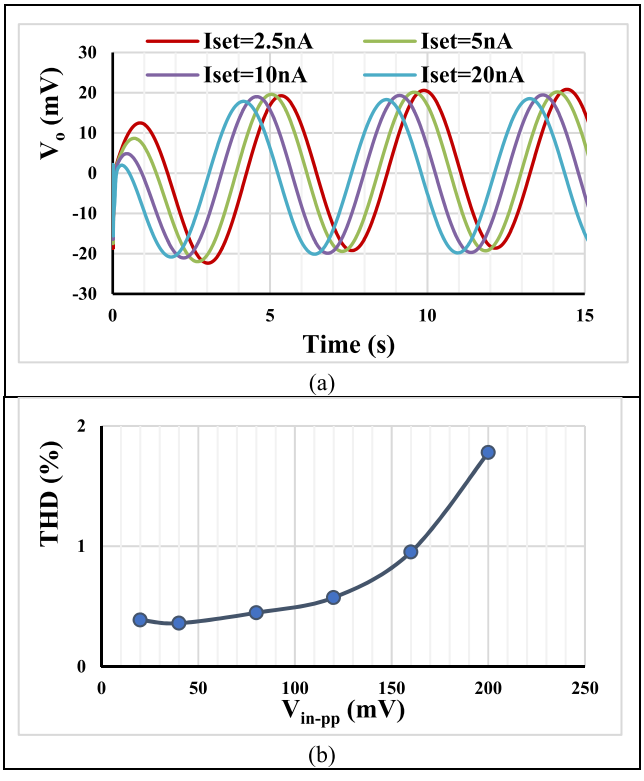

FIGURE 11. The transient response of the APF with different I_{set} (a) and the THD with different V_{in} (b).

It can see that the zero is located at origin, thus an ideal bandpass filter function can be obtained.

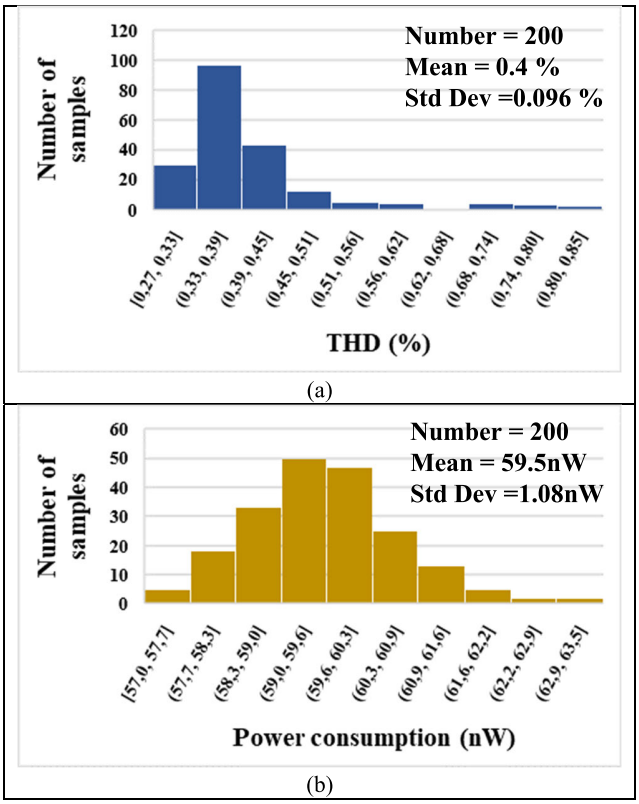

FIGURE 12. Histogram of the THD (a) and power consumption of the APF (b).

IV. POST-LAYOUT SIMULATION RESULTS

The circuit was designed in the Cadence platform and simulated with the Spectre simulator of the Analog Design Environment, using a 0.18 μm CMOS process from TSMC. The OTA transistor aspect ratios W/L (μm/μm) were: M_1, $M_2 = 2 \times 15.1$, M_3-$M_6 = 2 \times 10.1$, M_{3c}-M_{6c} = 10/1, M_7-M_{10}, $M_{13} = 2 \times 15.1$, M_{7c}-M_{10c}, M_{13c} = 15/1, M_{11}, M_{12} = 15/1, M_L =5/4 and the input metal-insulator-metal (MIM) capacitor C_{Bi} was 0.5 pF. The voltage supply is 0.5V ($\pm$0.25V for purpose of simulation), the bias voltage V_B is $-$100mV, and for setting current I_{set} = 10nA, the power consumption of the OTA is 29.77 nW. The layout of the MI-OTA is shown in Fig. 6 and the chip area is 0.01153 mm^2. The DC voltage gain of the MI-OTA was 31.17 dB, common mode rejection ratio was 90.05 and power supply rejection ratio was 37.26 dB [45].

Fig. 7 displays the OTA output current (a) and transconductance (b) as a function of the input voltage V_{in} for different values of the setting current I_{set} = (2.5, 5, 10, 20, 40) nA with 20pF load capacitance. The g_m varies from 1.65nS to 124nS and the high linearity is preserved within the range of $\pm$300mV regardless the I_{set}.

For the proposed voltage-mode first-order universal filter in Fig. 3, the capacitor was selected C_1 = 20 pF and the setting current $I_{set1} = I_{set2}$ = 10nA (g_m = 28.3nS) for designed cut-off frequency 222 Hz. The frequency responses

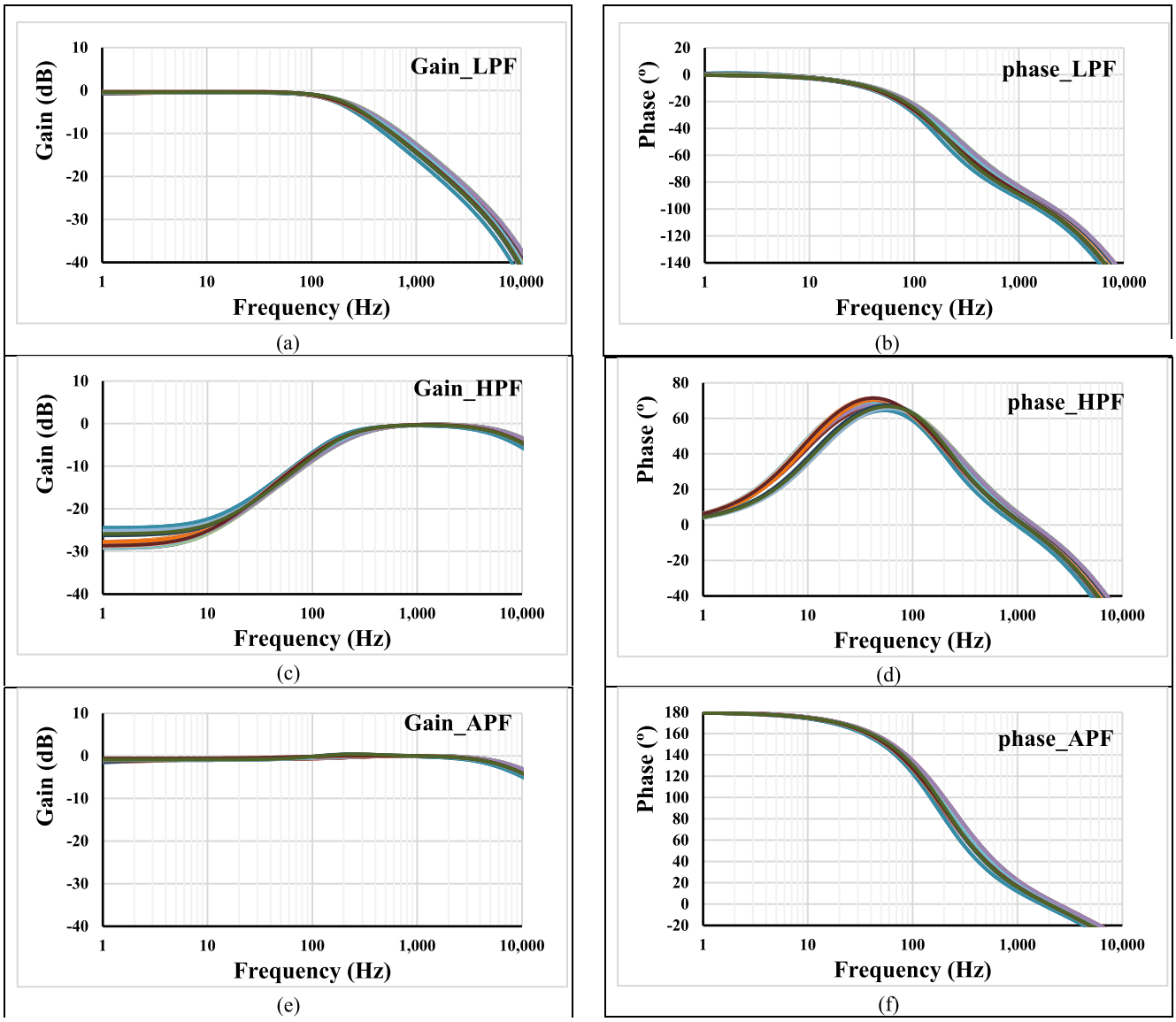

FIGURE 13. Frequency responses of gain and phase: (a,b) LPF; (c,d) HPF; (e,f) APF with PVT corners.

of the proposed filter for gain and phase are shown in Fig. 8. The simulated value of the cut-off frequency is observed to be 220 Hz and it is closed to the calculated one. Fig. 9 shows the frequency response of gain and phase with $I_{set2} = 10nA$ and different $I_{set} = I_{set1} = (2.5, 5, 10, 20, 40)$ nA. The cut-off frequency was 57 Hz, 112 Hz, 220 Hz, 430 Hz and 835 Hz, respectively.

Fig. 10 (a) shows the transient response of the APF with $I_{set1,2} = 10nA$ and applied sine wave input signal with $40mV_{pp}$@ 220Hz while (b) shows the spectrum of the output signal V_o using the Fast Fourier Transform (FFT). The total harmonic distortion was calculated as 0.36%. Fig. 11 (a) shows the transient response of the APF with $I_{set2} = 10nA$ and different setting current $I_{set1} = (2.5, 5, 10, 20)$ nA, the THD was around 0.36%. Fig. 11 (b) shows the THD of the APF with $I_{set1,2} = 10nA$ and different applied sine wave input signal @ 220Hz. The THD was below 1% for $160mV_{pp}$ input signal.

Fig. 12 shows the histogram of the THD (a) and power consumption (b) of the APF with $I_{set1,2} = 10nA$ and applied a sine wave input signal with $40mV_{pp}$@ 220Hz with 200 Monte Carlo analysis including mismatch and process variation. The mean value of the THD is 0.4% while the standard deviation is only 0.096%, the mean value of power consumption is 59.5nW and standard deviation is 1.08nW.

The Process, voltage and temperature corner analysis (PVT) was provided with $I_{set1,2} = 10nA$ as shown in Fig. 13. The process corners of the MOS transistors were fast-fast,

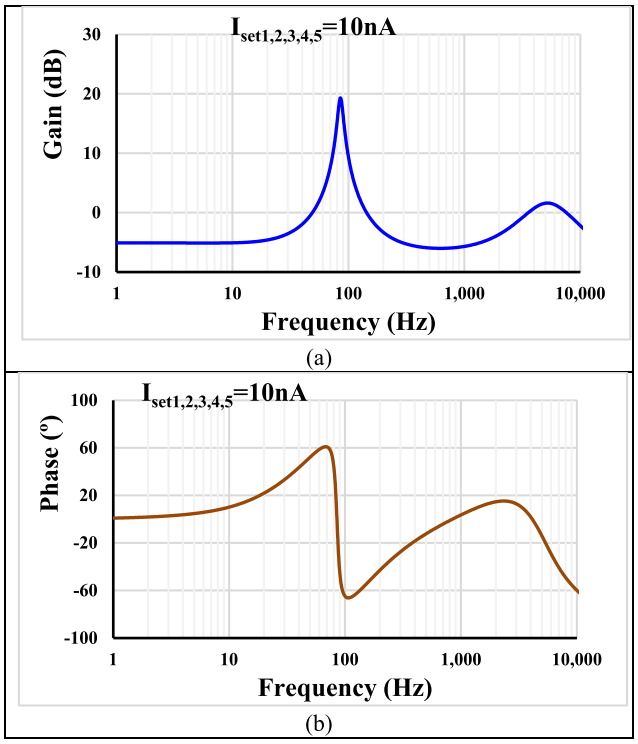

FIGURE 14. Frequency responses of gain (a) and phase (b) of the high-Q BPF.

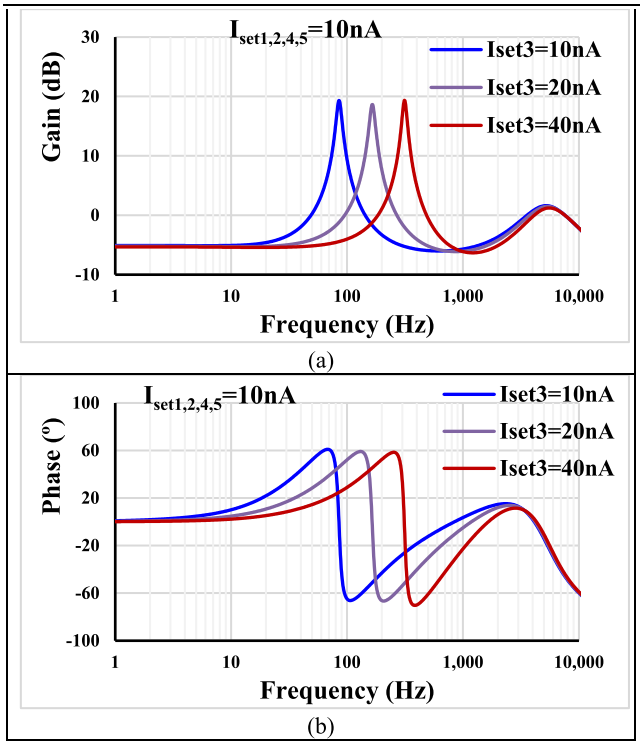

FIGURE 15. Frequency responses of gain (a) and phase (b) of the high-Q BPF when center frequency is tuned by I_{set3}.

slow-fast, fast-slow and slow-slow, the corners of the MIM capacitor were fast-fast and slow-slow, the voltage corners were $V_{DD}\pm10\%V_{DD}$, temperature corners were -20 °C and

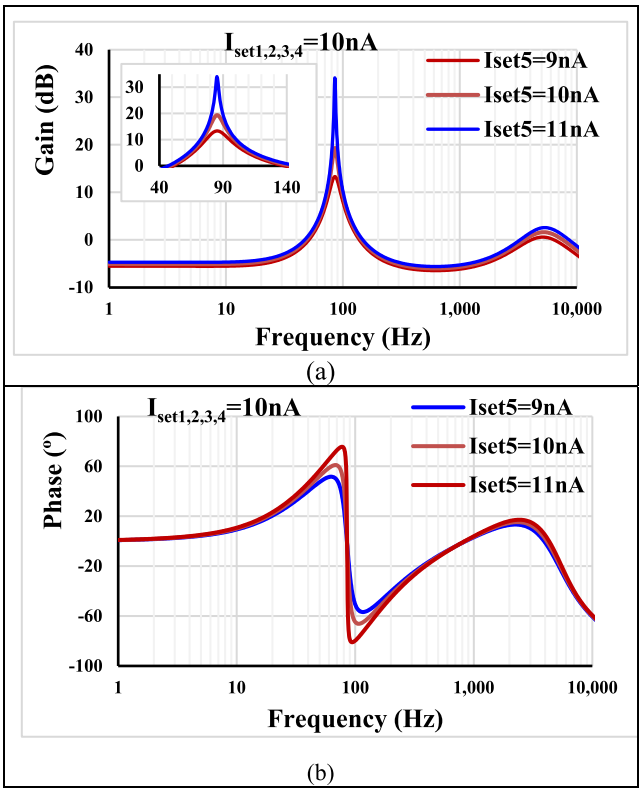

FIGURE 16. Frequency responses of gain (a) and phase (b) of the high-Q bandpass filter when Q is tuned by I_{set5}.

60 °C. As it is evident the curves are very closed to each other.

The proposed high-Q band-pass filter in Fig. 4 was simulated with $C_{1,2} = 50$pF, the $I_{set1,2,4,3,5} = 10$nA, the resistor value was chosen as $R = 1/g_m = 35.3$MΩ. The frequency and phase are shown in Fig. 14.

To confirm the tuning capability of the BPF, Fig. 15 shows the frequency responses of gain and phase when $I_{set1,2,4,5} = 10$nA and center frequency is tuned by $I_{set3} = (10, 20, 40)$nA. Fig. 16 shows the frequency responses of gain and phase when $I_{set1,2,3,4} = 10$nA and quality factor is tuned by $I_{set5} = (9, 10, 11)$ nA.

The proposed first-order filter has been compared with the previous works as shown in Table 2. The current-mode first-order filter in [14], some voltage-mode first-order filters [29], [30], [34], and mixed-mode first-order filter in [39] have been selected for comparison. The proposed filter offers six transfer functions like [14], but the filter in [14] uses multiple-output current ICCII which suffers from high power consumption. Compared to [29], [30], [34], and [39], the proposed filter offers more transfer functions and lower supply voltage and power consumption. Compared to [29] and [30], the proposed filter offers high-input impedance for all transfer functions. Compared to [14], [30], [34], and [39], this realization uses only grounded capacitor and devoid of passive resistor. The proposed filter is the only one that enjoys the lowest voltage supply and nW power consumption.

TABLE 2. Comparison table with previous first-order filters.

Features	Proposed	[14] 2017	[29] 2019	[30] 2021	[34] 2023	[39] 2023
Active and passive elements	2 OTA, 1 C	2 ICCII, 1 C, 1 MOS	2 OTA, 1 R, 2 C	1 LT1228, 2 R, 1 C	1 CFOA, 1 UGIA, 1 R, 1 C	1 VGA, 1 R, 1 C
Realization	CMOS structure (0.18 µm)	CMOS structure (0.13 µm)	CMOS structure (0.18 µm)	Commercial IC	CMOS structure (0.13 µm)	CMOS structure (0.18 µm)
Mode operation	VM	CM	VM	VM	VM	MM
Type of filter	MISO	SIMO	MISO	MISO	SIMO	MIMO
Number of filtering functions	6 (LP+, LP-, HP+, HP-, AP+, AP-)	6 (LP+, LP-, HP+, HP-, AP+, AP-)	3 (LP+, HP-, AP+)	4 (LP+, HP+, AP+, AP-)	3 (LP+, HP-, AP+)	3 (LP+, HP+, AP+)
High-input impedance	Yes	-	Yes	No	Yes	No
Using grounded capacitor/resistor	Yes	No	Yes	No	No	No
Pole frequency (kHz)	0.220	2600	8.05	90	7960	1590
Electronic control of parameter ω_o	Yes	Yes	Yes	Yes	No	Yes
Total harmonic distortion (%)	0.36 @40mV$_{pp}$	<1.5@90 µA$_{pp}$	-	1@200 mV$_{pp}$	1@120 mV$_{pp}$	-
Power supply voltages (V)	0.5	±0.75	±0.4	±5	±0.9	±0.9
Power consumption (µW)	59.5E-3	4080	47.2	57600	900	-
Verification of result	Post-layout Sim	Sim	Sim/Exp	Exp	Sim/Exp	Sim/Exp

Note: UIA = unity gain-inverting amplifier (UGIA), LP+= non-inverting low-pass filter, LP-= inverting low-pass filter, HP+= non-inverting high-pass filter, HP-= inverting high-pass filter, AP+= non-inverting all-pass filter, AP-= inverting all-pass filter, MISO = multiple-input signal-output, SIMO = single-input multiple-output, MM= Mixed-mode, ICCII= inverting second-generation current conveyors.

V. CONCLUSION

This paper presents a voltage-mode first-order universal filter using multiple-input OTAs. This work can express that multiple-input OTA can easily offer six transfer functions of first-order filters, namely three non-inverting transfer function of LPF, HPF, APF, and three inverting transfer function of LPF, HPF, APF into single topology. The proposed filter offers high-input impedance which is ideal for voltage-mode circuits. The pole frequency of all filters can be controlled electronically via the bias current. To show the advantages of the proposed filter, it has been used to realize a high-Q band-pass filter capable to work with extremely low voltage supply and with nano power consumption that make it suitable for modern nano-power portable electronics.

REFERENCES

[1] M. F. B. M. Idros and S. F. B. A. Hassan, "A design of Butterworth low pass filter's layout basideal filter approximation on the ideal filter approximation," in *Proc. IEEE Symp. Ind. Electron. Appl.*, Oct. 2009, pp. 754–757, doi: 10.1109/ISIEA.2009.5356355.

[2] U. Tietze, C. Schenk, and E. Gamm, *Electronic Circuits: Handbook for Design and Application*, 2nd ed. Cham, Switzerland: Springer, 2007.

[3] A. Toker, S. Ozoguz, O. Cicekoglu, and C. Acar, "Current-mode all-pass filters using current differencing buffered amplifier and a new high-Q bandpass filter configuration," *IEEE Trans. Circuits Syst. II, Analog Digit. Signal Process.*, vol. 47, no. 9, pp. 949–954, Sep. 2000, doi: 10.1109/82.868465.

[4] S. J. G. Gift, "The application of all-pass filters in the design of multiphase sinusoidal systems," *Microelectron. J.*, vol. 31, pp. 9–13, Jan. 2000, doi: 10.1016/S0026-2692(99)00084-1.

[5] Y.-A. Li, "A series of new circuits based on CFTAs," *AEU Int. J. Electron. Commun.*, vol. 66, no. 7, pp. 587–592, Jul. 2012, doi: 10.1016/j.aeue.2011.11.011.

[6] E. Yuce, S. Minaei, N. Herencsar, and J. Koton, "Realization of first-order current-mode filters with low number of Mos transistors," *J. Circuits, Syst. Comput.*, vol. 22, no. 1, Jan. 2013, Art. no. 1250071, doi: 10.1142/S0218126612500715.

[7] A. Kumar and S. K. Paul, "Current mode first order universal filter and multiphase sinusoidal oscillator," *AEU Int. J. Electron. Commun.*, vol. 81, pp. 37–49, Nov. 2017, doi: 10.1016/j.aeue.2017.07.004.

[8] B. Chaturvedi, J. Mohan, and A. Kumar, "A novel realization of current-mode first order universal filter," in *Proc. 6th Int. Conf. Signal Process. Integr. Netw. (SPIN)*, Noida, India, Mar. 2019, pp. 623–627, doi: 10.1109/SPIN.2019.8711629.

[9] J.-W. Horng, C.-M. Wu, J.-H. Zheng, and S.-Y. Li, "Current-mode first-order highpass, lowpass, and allpass filters using two ICCIIs," in *Proc. IEEE Int. Conf. Consum. Electron. Taiwan (ICCE-Taiwan)*, Sep. 2020, pp. 1–2, doi: 10.1109/ICCE-Taiwan49838.2020.9258111.

[10] F. Yucel, "A DVCC-based current-mode first-order universal filter," *J. Circuits, Syst. Comput.*, vol. 30, no. 16, Dec. 2021, Art. no. 2150305, doi: 10.1142/S0218126621503059.

[11] E. Yuce and S. Minaei, "A new first-order universal filter consisting of two ICCII + s and a grounded capacitor," *AEU Int. J. Electron. Commun.*, vol. 137, Jul. 2021, Art. no. 153802, doi: 10.1016/j.aeue.2021.153802.

[12] A. Raj, D. R. Bhaskar, R. Senani, and P. Kumar, "Extension of recently proposed two-CFOA-GC all pass filters to the realisation of first order universal active filters," *AEU Int. J. Electron. Commun.*, vol. 146, Mar. 2022, Art. no. 154119, doi: 10.1016/j.aeue.2022.154119.

[13] N. Herencsar, J. Koton, M. Sagbas, and U. E. Ayten, "New tunable resistorless CM first-order filter based on single CBTA and grounded capacitor," in *Proc. IEEE 59th Int. Midwest Symp. Circuits Syst. (MWSCAS)*, Abu Dhabi, United Arab Emirates, Oct. 2016, pp. 1–4, doi: 10.1109/MWSCAS.2016.7870064.

[14] L. Safari, E. Yuce, and S. Minaei, "A new ICCII based resistorless current-mode first-order universal filter with electronic tuning capability," *Microelectron. J.*, vol. 67, pp. 101–110, Sep. 2017, doi: 10.1016/j.mejo.2017.07.015.

[15] D. Agrawal and S. Maheshwari, "An active-C current-mode universal first-order filter and oscillator," *J. Circuits, Syst. Comput.*, vol. 28, no. 13, Dec. 2019, Art. no. 1950219, doi: 10.1142/S0218126619502190.

[16] B. Chaturvedi, A. Kumar, and J. Mohan, "Low voltage operated current-mode first-order universal filter and sinusoidal oscillator suitable for signal processing applications," *AEU Int. J. Electron. Commun.*, vol. 99, pp. 110–118, Feb. 2019, doi: 10.1016/j.aeue.2018.11.025.

[17] P. Singh, V. Varshney, A. Kumar, and R. K. Nagaria, "Electronically tunable first order universal filter based on CCDDCCTA," in *Proc. IEEE Conf. Inf. Commun. Technol.*, Dec. 2019, pp. 1–6, doi: 10.1109/CICT48419.2019.9066264.

[18] B. Chaturvedi, J. Mohan, and A. Kumar, "Resistorless realization of first-order current mode universal filter," *Radio Sci.*, vol. 55, no. 1, pp. 1–10, Jan. 2020, doi: 10.1029/2019RS006932.

[19] J. Mohan, B. Chaturvedi, and Jitender, "CMOS compatible first-order current mode universal filter structure and its possible tunable variant," *J. Circuits, Syst. Comput.*, vol. 31, no. 14, Sep. 2022, Art. no. 2250242, doi: 10.1142/S0218126622502425.

[20] A. Kumar, S. Kumar, D. H. Elkamchouchi, and S. Urooj, "Fully differential current-mode configuration for the realization of first-order filters with ease of cascadability," *Electronics*, vol. 11, p. 2072, Jul. 2022, doi: 10.3390/electronics11132072.

[21] I. Myderrizi, S. Minaei, and E. Yuce, "An electronically fine-tunable multi-input-single-output universal filter," *IEEE Trans. Circuits Syst. II, Exp. Briefs*, vol. 58, no. 6, pp. 356–360, Jun. 2011, doi: 10.1109/TCSII.2011.2158168.

[22] A. Abaci and E. Yuce, "Voltage-mode first-order universal filter realizations based on subtractors," *AEU Int. J. Electron. Commun.*, vol. 90, pp. 140–146, Jun. 2018, doi: 10.1016/j.aeue.2018.04.017.

[23] K. Banerjee, P. K. Bnadopadhyaya, B. Sarkar, and A. Biswas, "Multi input single output using operational transresistance amplifier as first order filter," in *Proc. IEEE VLSI Device Circuit Syst. (VLSI DCS)*, Jul. 2020, pp. 271–274, doi: 10.1109/VLSIDCS47293.2020.9179938.

[24] S. Kumari and D. Nand, "DDCC-based MISO type voltage-mode first-order universal filter," in *Proc. 2nd Int. Conf. Intell. Technol. (CONIT)*, Jun. 2022, pp. 1–6, doi: 10.1109/CONIT55038.2022.9847828.

[25] M. Dogan and E. Yuce, "A first-order universal filter including a grounded capacitor and two CFOAs," *Anal. Integr. Circuits Signal Process.*, vol. 112, pp. 379–390, Aug. 2022, doi: 10.1007/s10470-022-02021-2.

[26] K. Chinpark, W. Jaikla, S. Siripongdee, and P. Suwanjan, "Electronically controllable first-order multifuntion filter with using single active building block," in *Proc. 3rd Int. Conf. Control Robot. Eng. (ICCRE)*, Apr. 2018, pp. 192–195, doi: 10.1109/ICCRE.2018.8376462.

[27] P. Singh, V. Varshney, A. Kumar, and R. K. Nagaria, "Electronically tunable first order universal filter based on CCDDCCTA," in *Proc. IEEE Conf. Inf. Commun. Technol.*, Allahabad, India, Dec. 2019, pp. 1–6, doi: 10.1109/CICT48419.2019.9066264.

[28] P. Moonmuang, T. Pukkalanun, and W. Tangsrirat, "Voltage differencing buffered amplifier-based electronically tunable grounded capacitance multiplier," in *Proc. 8th Int. Conf. Informat., Environ., Energy Appl.*, Mar. 2019, pp. 208–211, doi: 10.1145/3323716.3323740.

[29] W. Jaikla, P. Talabthong, S. Siripongdee, P. Supavarasuwat, P. Suwanjan, and A. Chaichana, "Electronically controlled voltage mode first order multifunction filter using low-voltage low-power bulk-driven OTAs," *Microelectron. J.*, vol. 91, pp. 22–35, Sep. 2019, doi: 10.1016/j.mejo.2019.07.009.

[30] W. Jaikla, U. Buakhong, S. Siripongdee, F. Khateb, S. Sotner, P. Silapan, P. Suwanjan, and A. Chaichana, "Single commercially available IC-based electronically controllable voltage-mode first-order multifunction filter with complete standard functions and low output impedance," *Sensors*, vol. 21, no. 21, p. 7376, 2021, doi: 10.3390/s21217376.

[31] G. Barile, L. Safari, L. Pantoli, V. Stornelli, and G. Ferri, "Electronically tunable first order AP/LP and LP/HP filter topologies using electronically controllable second generation voltage conveyor (CVCII)," *Electronics*, vol. 10, p. 822, Mar. 2021, doi: 10.3390/electronics10070822.

[32] D. Duangmalai and P. Suwanjan, "The voltage-mode first order universal filter using single voltage differencing differential input buffered amplifier with electronic controllability," *Int. J. Electr. Comput. Eng.*, vol. 12, pp. 1308–1323, Apr. 2022, doi: 10.11591/ijece.v12i2.pp1308-1323.

[33] P. Singh and R. K. Nagaria, "Voltage mode and trans-admittance mode first-order universal filters employing DV-EXCCCII," *Austral. J. Electr. Electron. Eng.*, vol. 19, no. 4, pp. 396–406, Oct. 2022, doi: 10.1080/1448837X.2022.2088571.

[34] M. Dogan, E. Yuce, and Z. Dicle, "CFOA-based first-order voltage-mode universal filters," *AEU Int. J. Electron. Commun.*, vol. 161, Mar. 2023, Art. no. 154550, doi: 10.1016/j.aeue.2023.154550.

[35] B. Chaturvedi and A. Kumar, "Electronically tunable first-order filters and dual-mode multiphase oscillator," *Circuits, Syst., Signal Process.*, vol. 38, pp. 2–25, Jan. 2019, doi: 10.1007/s00034-018-0849-x.

[36] K. Rohilla, K. L. Pushkar, R. Kumar, and A. Raj, "Resistorless first-order universal filter structures employing OTAs with independent controllability of gain and pole frequency," *IETE J. Res.*, pp. 1–21, Oct. 2022, doi: 10.1080/03772063.2022.2132305.

[37] A. Raj, "Mixed-mode electronically-tunable first-order universal filter structure employing operational transconductance amplifiers," *J. Circuits, Syst. Comput.*, vol. 31, no. 13, Sep. 2022, Art. no. 2250234, doi: 10.1142/S0218126622502346.

[38] D. R. Bhaskar, A. Raj, S. Rajb, and P. Kumar, "CFOA-based simple mixed-mode first-order universal filter configurations," *Int. J. Circuit Theory Appl.*, vol. 50, pp. 264–2631, Jul. 2022, doi: 10.1002/cta.3289.

[39] N. Roongmuanpha, N. Likhitkitwoerakul, M. Fukuhara, and W. Tangsrirat, "Single VDGA-based mixed-mode electronically tunable first-order universal filter," *Sensors*, vol. 23, p. 2759, Mar. 2023, doi: 10.3390/s23052759.

[40] M. Kumngern, "Electronically tunable current-mode all-pass filter-based high-Q bandpass filter using minimum elements," in *Proc. TENCON IEEE Region 10 Conf.*, Singapore, Jan. 2009, pp. 1–4, doi: 10.1109/TENCON.2009.5396215.

[41] W. Tangsrirat, W. Tanjaroen, and T. Pukkalanun, "Current-mode multiphase sinusoidal oscillator using CDTA-based allpass sections," *AEU Int. J. Electron. Commun.*, vol. 63, no. 7, pp. 616–622, Jul. 2009, doi: 10.1016/j.aeue.2008.05.001.

[42] W. Jaikla and P. Prommee, "Electronically tunable current-mode multiphase sinusoidal oscillator employing CCCDTA-based allpass filters with only grounded passive elements," *Radioengineering*, vol. 20, no. 3, pp. 594–599, 2011.

[43] A. Wyszynski and R. Schaumann, "Using multiple-input transconductors to reduce number of components in OTA-C filter design," *Electron. Lett.*, vol. 28, pp. 217–220, Jan. 1992, doi: 10.1049/el:19920135.

[44] M. Kumngern, N. Aupithak, F. Khateb, and T. Kulej, "0.5 V fifth-order Butterworth low-pass filter using multiple-input OTA for ECG applications," *Sensors*, vol. 20, p. 7343, Dec. 2020, doi: 10.3390/s20247343.

[45] F. Khateb, T. Kulej, M. Akbari, and K. Tang, "A 0.5-V multiple-input bulk-driven OTA in 0.18-μm CMOS," *IEEE Trans. Very Large Scale Integr. (VLSI) Syst.*, vol. 30, no. 11, pp. 1739–1747, Nov. 2022, doi: 10.1109/TVLSI.2022.3203148.

[46] F. Krummenacher and N. Joehl, "A 4-MHz CMOS continuous-time filter with on-chip automatic tuning," *IEEE J. Solid-State Circuits*, vol. SSC-23, no. 3, pp. 750–758, Jun. 1988.

[47] P. M. Furth and A. G. Andreou, "Linearised differential transconductors in subthreshold CMOS," *Electron. Lett.*, vol. 31, no. 7, pp. 545–547, Mar. 1995.

[48] M. Kumngern, F. Khateb, T. Kulej, and C. Psychalinos, "Multiple-input universal filter and quadrature oscillator using multiple-input operational transconductance amplifiers," *IEEE Access*, vol. 9, pp. 56253–56263, 2021.

[49] D. T. Comer, D. J. Comer, and J. R. Gonzalez, "A high-frequency integrable bandpass filter configuration," *IEEE Trans. Circuits Syst. II, Analog Digit. Signal Process.*, vol. 44, no. 10, pp. 856–861, Oct. 1997, doi: 10.1109/82.633445.

FABIAN KHATEB received the M.Sc. degree in electrical engineering and communication, the M.Sc. degree in business and management, the Ph.D. degree in electrical engineering and communication, and the Ph.D. degree in business and management from the Brno University of Technology, Czech Republic, in 2002, 2003, 2005, and 2007, respectively. He is currently a Professor with the Department of Microelectronics, Faculty of Electrical Engineering and Communication, Brno University of Technology; the Department of Electrical Engineering, University of Defence, Brno; and the Department of Information and Communication Technology in Medicine, Faculty of Biomedical Engineering, Czech Technical University in Prague. He holds five patents. He has authored or coauthored more than 100 publications in journals and proceedings of international conferences. His expertise is in new principles of designing low-voltage low-power analog circuits, particularly for biomedical applications. He is a member of the Editorial Board of the *Microelectronics Journal*, *Sensors*, *Electronics*, and *Journal of Low Power Electronics and Applications*. He is an Associate Editor of IEEE Access, *Circuits, Systems and Signal Processing*, *IET Circuits, Devices and Systems*, and *International Journal of Electronics*. He was a Lead Guest Editor for the Special Issues on Low Voltage Integrated Circuits and Systems of the *Circuits, Systems and Signal Processing*, in 2017, *IET Circuits, Devices and Systems*, in 2018, and *Microelectronics Journal*, in 2019. He was also a Guest Editor for the Special Issue on Current-Mode Circuits and Systems: Recent Advances, Design and Applications of the *International Journal of Electronics and Communications*, in 2017.

MONTREE KUMNGERN received the B.S.Ind.Ed. degree in electrical engineering from the King Mongkut's University of Technology Thonburi, Thailand, in 1998, and the M.Eng. and D.Eng. degrees in electrical engineering from the King Mongkut's Institute of Technology Ladkrabang, Thailand, in 2002 and 2006, respectively. In 2007, he was a Lecturer with the Department of Telecommunications Engineering, Faculty of Engineering, King Mongkut's Institute of Technology Ladkrabang, where he was an Assistant Professor, from 2010 to 2017, and is currently an Associate Professor. He has authored or coauthored more than 200 publications in journals and proceedings of international conferences. His research interests include analog and digital integrated circuits, discrete-time analog filters, non-linear circuits, data converters, and ultra-low voltage building blocks for biomedical applications.

TOMASZ KULEJ received the M.Sc. and Ph.D. degrees from the Gdańsk University of Technology, Gdańsk, Poland, in 1990 and 1996, respectively. He was a Senior Design Analysis Engineer with Chipworks Inc., Polish Branch, Ottawa, Canada. He is currently an Associate Professor with the Department of Electrical Engineering, Częstochowa University of Technology, Poland, where he conducts lectures on electronics fundamentals, analog circuits, and computer aided designs. He has authored or coauthored more than 90 publications in peer-reviewed journals and conferences. He holds three patents. His research interests include analog integrated circuits in CMOS technology, with emphasis on low-voltage and low-power solutions. He serves as an Associate Editor for the *Circuits Systems and Signal Processing* and *IET Circuits Devices and Systems*. He was also a Guest Editor for the Special Issues on Low Voltage Integrated Circuits of the *Circuits Systems and Signal Processing*, in 2017, *IET Circuits Devices and Systems*, in 2018, and *Microelectronics Journal*, in 2019.